



INFLUENCE OF SHEAR-BANDING EFFECTS ON THE ULTIMATE BEARING CAPACITY EQUATION OF FOUNDATIONS

Tse-Shan Hsu

President, Institute of Mitigation for Earthquake Shear Banding Disasters

Professor, Feng-Chia University, Taiwan, R.O.C., tshsu@fcu.edu.tw

Da-Jie Lin, Tsai-Fu Chuang and Yi-Min Huang

Associate Professors and Assistant Professor, Feng-Chia University, Taiwan, R.O.C.

Abstract

Previous research has shown that the sliding failure plane of foundations in terms of shear banding can only be induced by plastic strain softening. Shear banding is also considered a failure phenomenon that appears under the condition of structural instability. Based on the research results of this study, four conclusions can be drawn as follows: (1) The solution of shear bands comes from the determinant of the structure matrix being equal to zero, so it can be obtained by the finite-element method under prescribed displacements. (2) Under the condition that the initial structure is symmetric, the structure will lose its symmetry when shear bands are induced by plastic strain softening. (3) In the derivation of the ultimate bearing capacity equation of foundations, if a perfectly plastic model is adopted after setting the general shear failure plane, then a shear band is not induced and the structural symmetry is maintained, resulting in overestimation of the ultimate bearing capacity of the foundations. (4) Traditional scholars adopt the perfectly plastic model; thus, shear bands cannot be induced and the plastic zones spread to the elastic zones originally outside the shear bands, resulting in overestimation of the ultimate bearing capacity of foundations. Therefore, the authors suggest that the strain-softening model should be adopted in future studies on the ultimate bearing capacity of foundations. Design codes should also introduce the ultimate bearing capacity equation of foundations

based on the strain-softening model to ensure the safety of building foundations.

Keywords: strain softening, perfectly plastic, ultimate bearing capacity, foundation, general shear failure, punching shear failure, stability, symmetry.

Introduction

The design of foundations for residential buildings requires the ultimate bearing capacity of the soil. The literature shows that scholars have used many different methods to study the ultimate bearing capacity of foundations (Bolton and Lau, 1993; Davis and Booker, 1971; Chen, 1975; Chi and Lin, 2020; Peng and Peng, 2020; Griffiths, 1982; Sokolovskii, 1965). These methods include the limit equilibrium method, the slip-line method, the limit analysis method, the numerical limit analysis method, the finite-element method, and the finite-difference

method.

The earliest research works by Prandtl (1920) and Reissner (1924) derived the ultimate bearing capacity equation for foundations using soil plasticity. The extended research results of Terzaghi (1943), which are widely quoted in textbooks (Bowles, 1988; Das, 1983; McCarthy, 2007; You, 1974), adopted the rigid-perfectly plastic model shown in Figure 1, and the symmetrical long-strip foundation shown in Figure 2 with symmetrical shear failure surfaces under plane strain conditions.

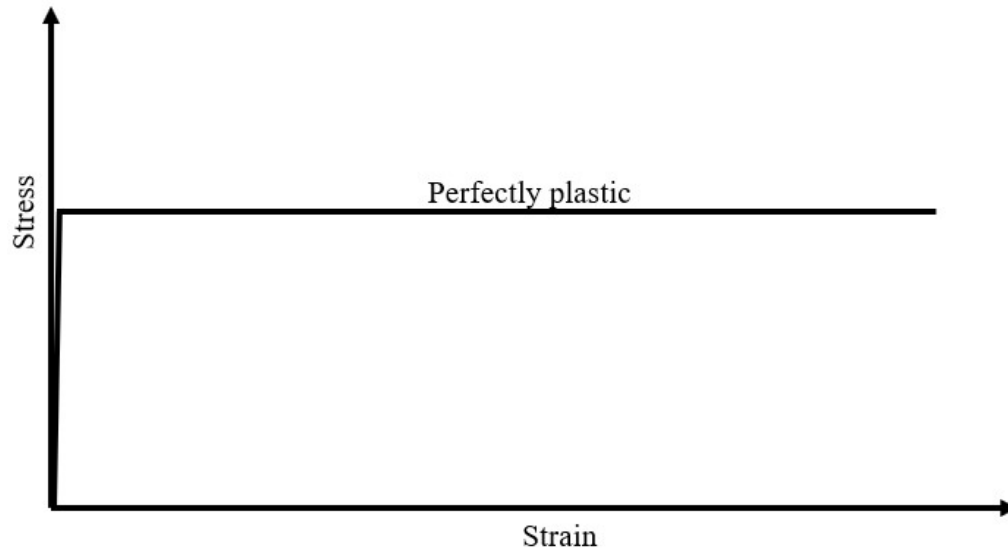


Figure 1. The soil model used by Terzaghi to derive the ultimate bearing capacity equation (Terzaghi, 1943).

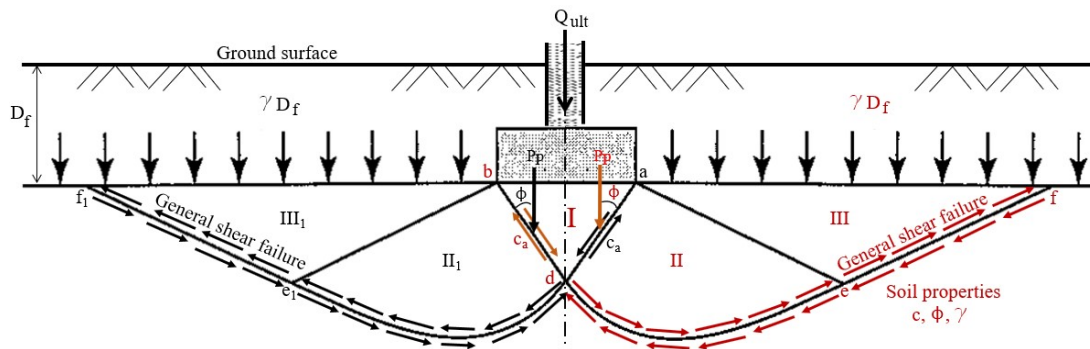


Figure 2. The general shear failure plane set before deriving the ultimate bearing capacity equation of the foundation (reproduced from Terzaghi, 1943).

However, in the load test of a foundation on a level ground surface (see Figure 3), when the soil layer is a firm clay layer or a dense sand layer,

McCarthy (2007) presented the general shear failure shown in Figure 4 and the load–settlement curve shown in Figure 5.

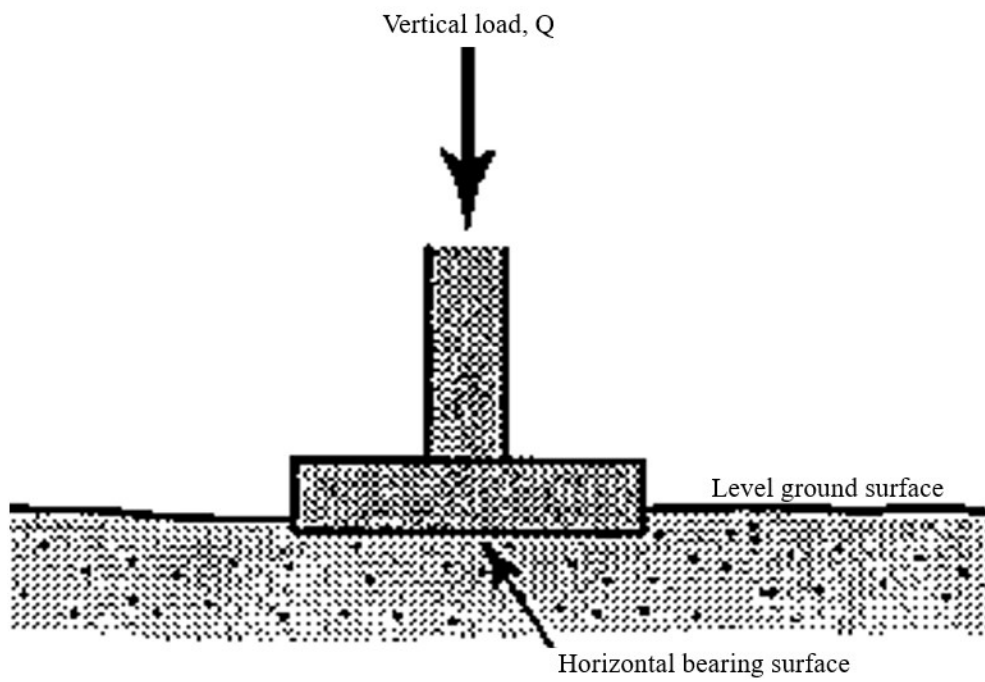


Figure 3. Typical load test for a strip footing (McCarthy, 2007).

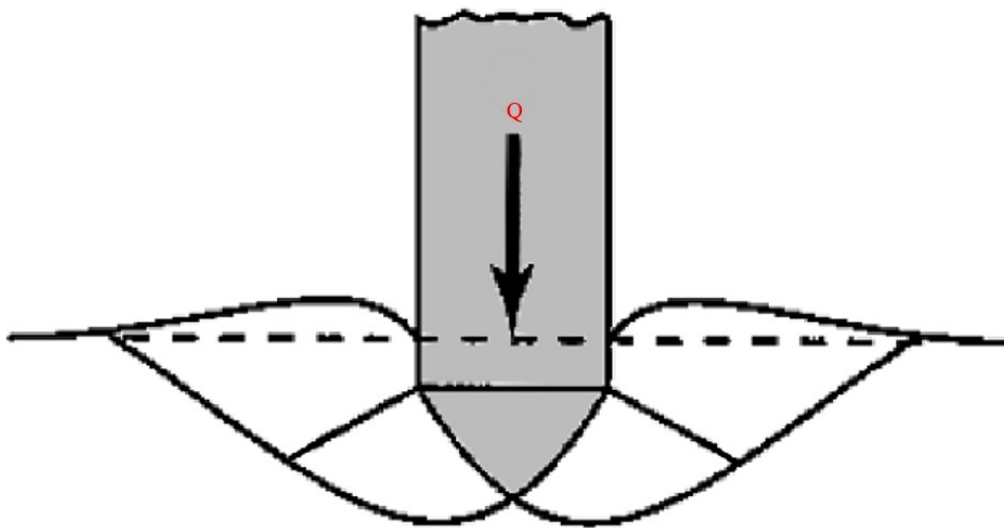


Figure 4. General shear failure of a strip footing (McCarthy, 2007).

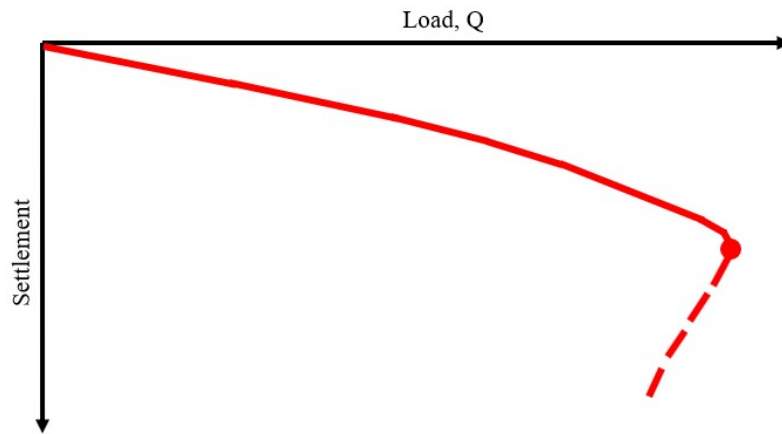


Figure 5. Load–settlement curve for general shear failure of a strip footing (reproduced from McCarthy, 2007).

For a soft clay layer or a loose sand layer, McCarthy (2007) obtained the punching shear failure shown in

Figure 6, and the load–settlement curve shown in Figure 7.

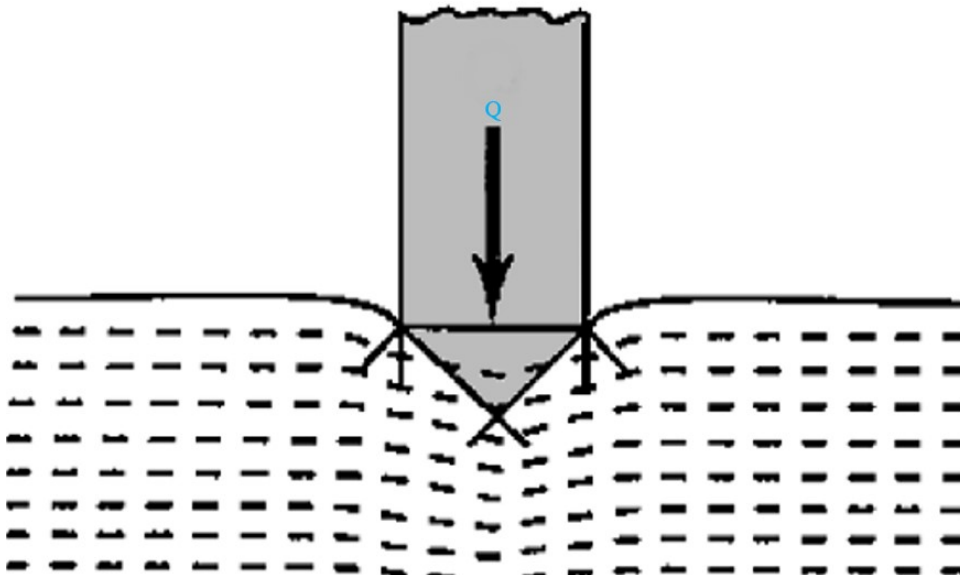


Figure 6. Punching shear failure of a strip footing (McCarthy, 2007).

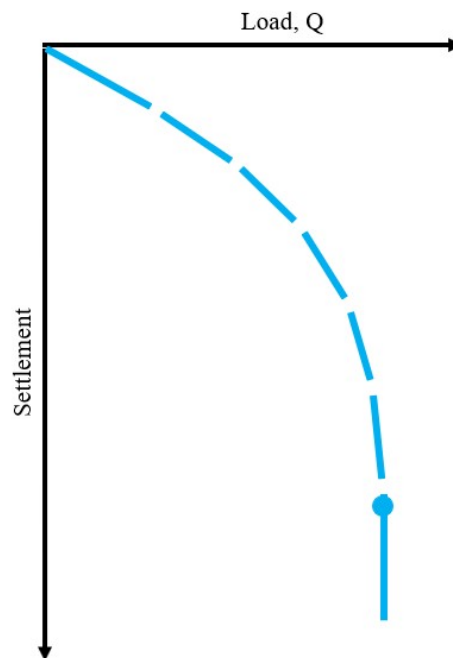


Figure 7. Load–settlement curve for punching shear failure of a strip footing (reproduced from McCarthy, 2007).

McCarthy (2007) showed that general shear failure occurs in a firm clay layer or dense sand layer, and that punching shear failure occurs in a soft clay layer or loose sand layer. Furthermore, McCarthy (2007) also showed that when general shear failure occurs, the load–settlement curve is plastic strain softened (see Figure 5); conversely, when punching shear failure occurs, the load–settlement curve is perfectly plastic (see Figure 7). However, Figure 2 shows that in the process of deriving the ultimate bearing capacity equation, Terzaghi adopted the incompatible perfectly plastic model when the general shear failure plane

was first set. Therefore, it is necessary to further explore the ultimate bearing capacity equation for foundations as derived by Terzaghi.

Localizations of Deformations in Strain-Softening Plasticity

It is generally noted that when ductile solids such as rocks, overly consolidated clays, granular materials, polymers, and structural metals are deformed sufficiently far into the plastic range, a smoothly and continuously varying deformation pattern gives way to highly localized deformations in the form of shear bands (Rice, 1977). Such

a phenomenon can be understood as instability in the macroscopic constitutive description of the inelastic deformation of the material. Specifically, instability can be understood in the way that the constitutive relations allow the homogeneous deformation of an initially uniform material to lead to a bifurcation point, at which nonuniform deformation can be initiated in a planar

band under conditions of continuing equilibrium and continuing homogeneous deformation outside the zone of localization (Rudnicki and Rice, 1975).

The Constitutive Equation

For strain-softening plasticity, the yield function, F , proposed by Hsu (1987), is expressed as follows:

$$F = J_{2D}^{1/2} - (\kappa + H\gamma_{oct}^p) = 0, \quad (\text{Equation 1})$$

where:

J_{2D} = the second invariant of deviatoric stress,

κ = the size of the initial yield surface,

γ_{oct}^p = the plastic octahedral shear strain, and

H = the strain-softening parameter.

Differentiating Equation 1 leads to:

$$dF = \left(\frac{\partial F}{\partial \underline{\sigma}}\right)^T d\underline{\sigma} + \left(\frac{\partial F}{\partial \gamma_{oct}^p}\right)^T d\gamma_{oct}^p = \left(\frac{\partial F}{\partial \underline{\sigma}}\right)^T d\underline{\sigma} - Hd\gamma_{oct}^p = 0, \quad (\text{Equation 2})$$

where:

$d\underline{\sigma}$ = the incremental stress vector and

$d\gamma_{oct}^p$ = the incremental plastic octahedral shear strain.

The flow rule is:

$$d\underline{\varepsilon}^p = \lambda \frac{\partial F}{\partial \underline{\sigma}} = \lambda \left(\frac{1}{2} J_{2D}^{-1/2} \underline{S}\right).$$

Therefore, the elastic–plastic strain-softening stress–strain matrix can

be derived as follows:

$$\begin{aligned} \underline{D}^{ep} &= \underline{D}^e - \underline{D}^p \\ &= \underline{D}^e - \underline{D}^e \left(\frac{\partial F}{\partial \underline{\sigma}} \right)^T \frac{\partial F}{\partial \underline{\sigma}} \underline{D}^e \left[\frac{1}{\sqrt{6}} H + \left(\frac{\partial F}{\partial \underline{\sigma}} \right)^T \underline{D}^e \frac{\partial F}{\partial \underline{\sigma}} \right]^{-1} \end{aligned}$$

Condition for Stability of the Solution

For plastic strain-softening materials, two types of energy—the incremental plastic strain energy and damage energy—are dissipated during a load step in the strain-softening range. The incremental plastic energy of an element for a particular stress incre-

ment is equal to the shaded area below the stress–strain curve, as shown in Figure 8, times the volume of the element. The incremental damage energy of an element for a particular load step is equal to the shaded area above the stress–strain curve, as shown in Figure 8, times the volume of the element.

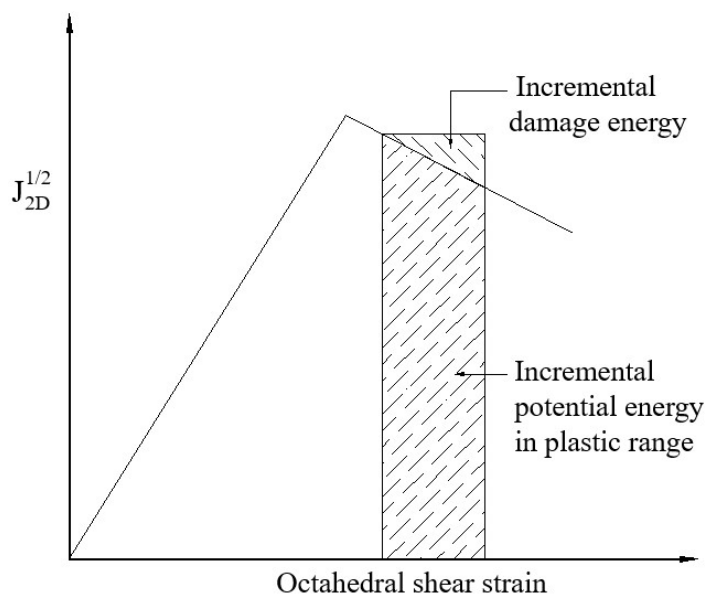


Figure 8. Schematic diagram of the incremental damage energy and the incremental plastic energy.

In reviewing the stability of the incremental finite-element solutions,

which include strain-softening material behavior, Prevost (1974) used the

variational approach based on the internal strain energy due to the stresses of the existing state and the stress increments to obtain the failure mechanism, which he defined as follows: “A failure mechanism develops when the incremental external work put into the system, plus the incremental work reduced by the plastic, strain-softening zone, equals or exceeds the work that may be absorbed by the surrounding unyielded and/or strain-hardening material.” The volume, V of the body can then be divided into two sub-volumes, V_{ps} and $V - V_{ps}$, where V_{ps} is the total volume of the strain-softening regions. Under this consideration, the uniqueness of the incremental solutions is proved.

Based on the physical behavior of materials, it is generally accepted that if the total external incremental applied

energy is positive, then the total induced internal incremental strain energy must be positive. On the other hand, if the total external incremental applied energy is negative, then the total induced internal incremental strain energy must also be negative. Any numerical solution must obey such a law; otherwise, the solutions will be unstable. The above criterion has been used in this research for determining the stability condition of the incremental solutions.

In a variational approach, the total potential energy π_p is used in static elastic analyses. Therefore, the total incremental potential energy, $d\pi_p$ should be used in the derivation of the equilibrium equation for the incremental load condition. The total incremental potential energy is:

$$d\pi_p = (\text{Total incremental potential energy due to existing loads and the corresponding induced internal stresses}) + (\text{Total incremental potential energy due to the external load increments and the corresponding induced internal stress increments})$$

$$= \left(\int_V \underline{\sigma}^T d\underline{\varepsilon} dV - \sum d\underline{u}^T \underline{F} \right) + \left(\frac{1}{2} \int_V d\underline{\sigma}^T d\underline{\varepsilon} dV - \sum d\underline{u}^T d\underline{F} \right), \quad (\text{Equation 3})$$

where:

- $\underline{\sigma}$ = the existing stress vector,
- $d\underline{\sigma}$ = the incremental stress vector,
- $d\underline{\varepsilon}$ = the incremental strain vector,
- $d\underline{u}$ = the incremental displacement vector,

\underline{F} = the existing force vector, and
 $d\underline{F}$ = the incremental force vector.

Since the structure should be in equilibrium under a set of existing forces, it can be concluded that the first term on the right-hand side of Equation 3 will disappear for the existing forces, *i.e.*, the existing forces will contribute no incremental potential energy. How-

ever, the incremental forces, which include body force, surface tractions, and applied concentrated forces, will produce some incremental potential energy. Therefore, the total incremental potential energy becomes:

$$d\pi_p = \frac{1}{2} \int_V d\underline{\sigma}^T d\underline{\varepsilon} dV - \sum d\underline{u}^T d\underline{F}. \quad (\text{Equation 4})$$

In the finite-element approximation, Equation 4 can be expressed as follows:

$$d\pi_p = \frac{1}{2} \int_V d\underline{u}^T \underline{B}^T \underline{D}^{*p} \underline{B} d\underline{u} dV - \sum d\underline{u}^T d\underline{F}, \quad (\text{Equation 5})$$

where

\underline{B} = the strain-displacement matrix.

The global stiffness matrix \underline{K} is:

$$\underline{K} = \int_V \underline{B}^T \underline{D}^{*p} \underline{B} dV. \quad (\text{Equation 6})$$

Substitution of Equation 6 into 5 leads to:

$$d\pi_p = \frac{1}{2} d\underline{u}^T \underline{K} d\underline{u} - d\underline{u}^T d\underline{F}. \quad (\text{Equation 7})$$

It can be seen from Equation 7 that, for the condition of prescribed displacements, since all of the forces are induced, both terms on the right

side of Equation 7 always have the same sign. This means that the condition of stability for the incremental solutions for the prescribed displacement

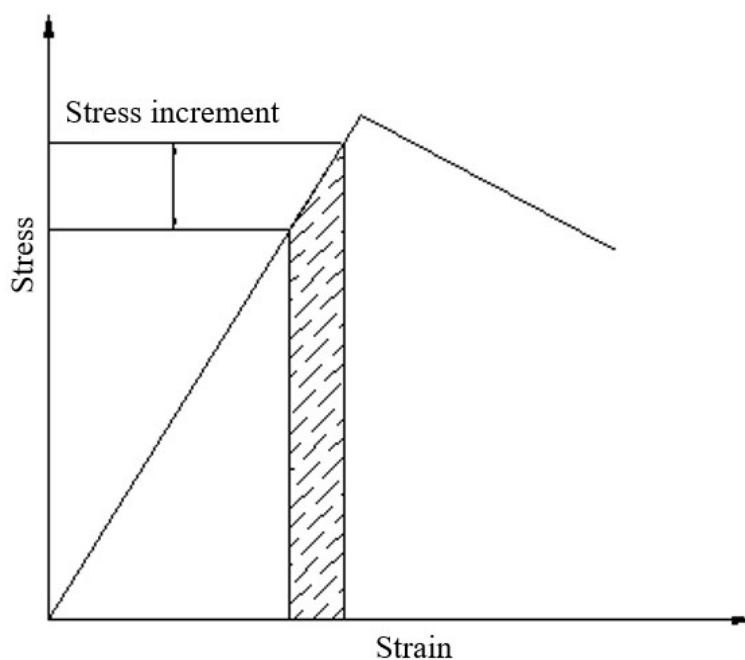
case is guaranteed. When the forces are prescribed and if the total external incremental energy is positive, the stability of the incremental solutions is guaranteed only when the global stiffness matrix is positive definite. When the global stiffness matrix is negative definite, the instability condition of the solution will occur.

Condition for Uniqueness of the Solution

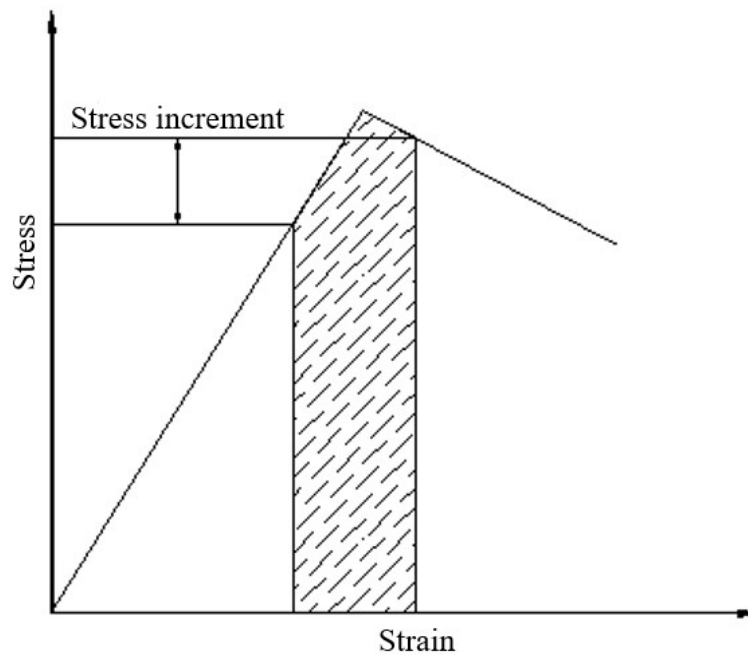
For a strain-hardening material or perfectly plastic material, Drucker's postulate is the required condition for

uniqueness of the solution. According to Drucker's postulate, the required condition for uniqueness of the solution is that the two potential energy increments on the right-hand side of Equation 7 are both positive.

For the strain-softening material, the solution can be unique even with the negative net potential energy produced by the external agencies. It has been argued that two solutions can be obtained if there is more than one minimum of the total incremental potential energy, as shown in Figure 9.



(a) Without damage energy

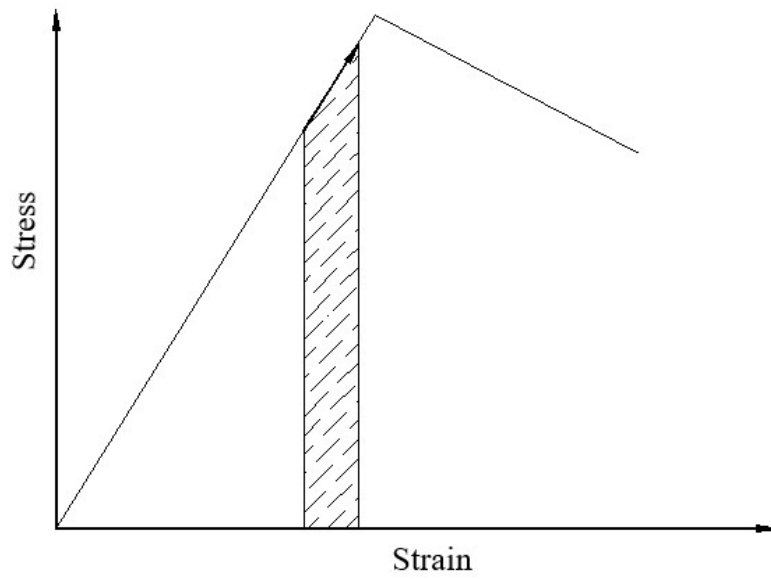


(b) With damage energy

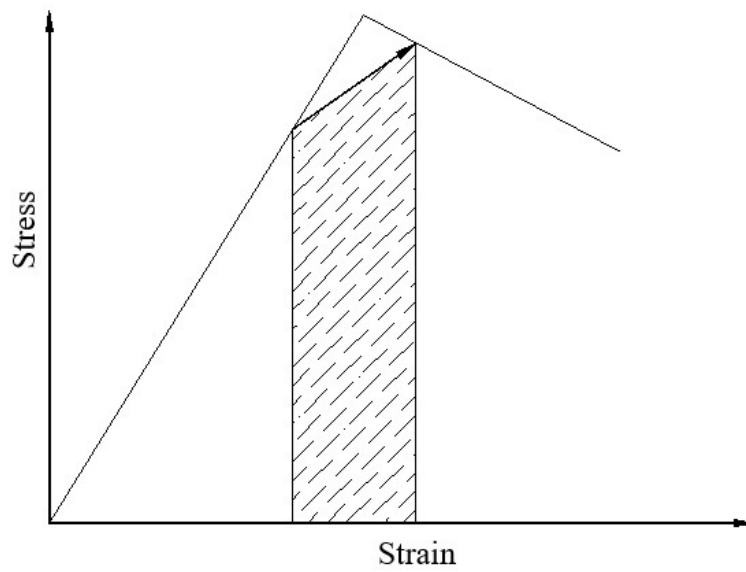
Figure 9. Two solutions for two minimum total incremental potential energies for a stress increment (Hsu, 1987).

However, as explained in Figure 10, there is only one minimum total incremental potential energy. This is because the average of the stress-strain matrix for the existing stresses ($\underline{\sigma}$) and the existing stresses plus the stress in-

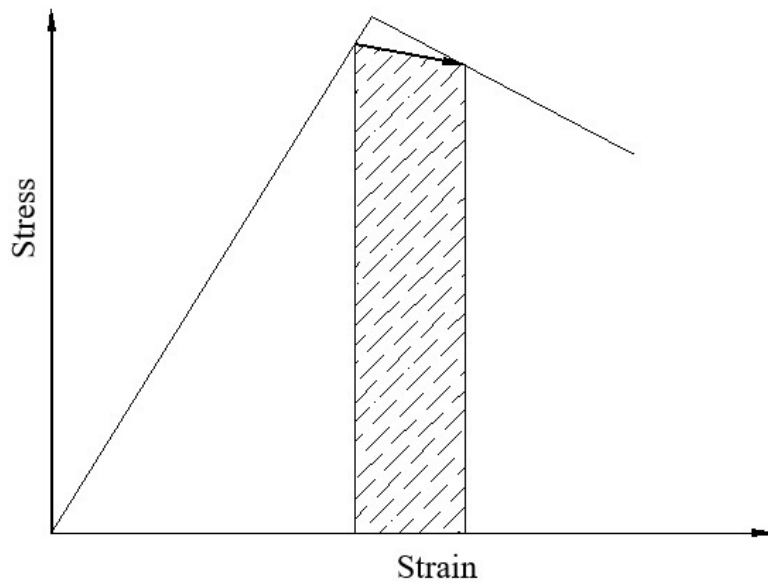
crements ($\underline{\sigma} + d\underline{\sigma}$) are used to form the global stiffness matrix. As shown in Figure 10, only one of the four conditions will be used; hence, only one minimum total incremental potential energy will exist.



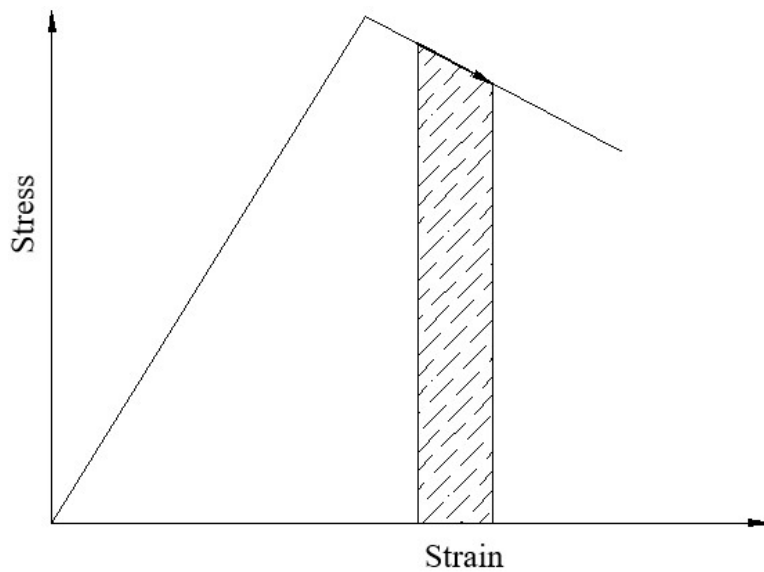
(a) Elastic range



(b) Elastic-plastic range



(c) Elastic-plastic range



(d) Plastic range

Figure 10. Four possible conditions in a stress increment when an averaging scheme is used to form the stress-strain matrix (Hsu, 1987).

For uniqueness, two sets of solutions, \underline{du}_1 and \underline{du}_2 , are assumed to satisfy the equilibrium condition at the same time. The equilibrium condition is derived by minimizing the total incremental potential energy; therefore, both \underline{du}_1 and \underline{du}_2 should provide the same

minimum total incremental potential energy. By substituting \underline{du}_1 and \underline{du}_2 into Equation 7 and minimizing the total incremental potential energy with respect to \underline{du}_1 and \underline{du}_2 , one will obtain:

$$\underline{K}\underline{du}_1 = \underline{dF} \quad \text{and} \quad \text{(Equation 8)}$$

$$\underline{K}\underline{du}_2 = \underline{dF}. \quad \text{(Equation 9)}$$

Equations 8 and 9 can be combined as follows:

$$\underline{K}(\underline{du}_1 - \underline{du}_2) = \underline{0}. \quad \text{(Equation 10)}$$

Therefore, one of the following two conditions must be true:

$$\underline{du}_1 = \underline{du}_2 \quad \text{(Equation 11)}$$

or

$$\det(\underline{K}) = 0. \quad \text{(Equation 12)}$$

For elastic–plastic strain-hardening materials or elastic–perfectly plastic materials, the determinant of the structural stiffness ma-

trix $\det(\underline{K})$ cannot be equal to zero, so $\underline{du}_1 = \underline{du}_2$. In this case, the analysis result does not include shear bands (see Figures 11 and 12).

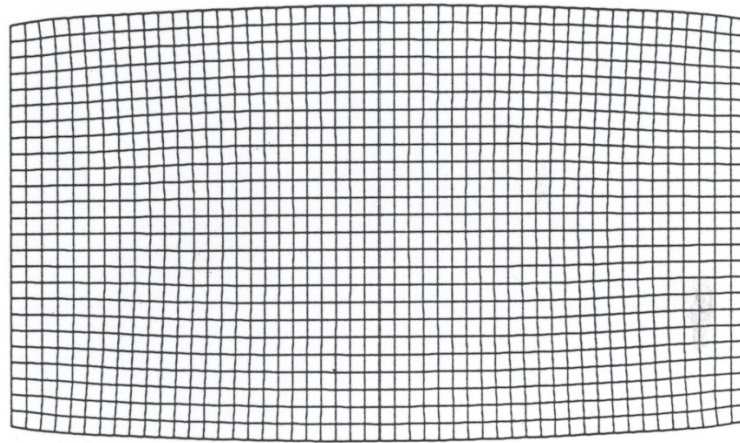


Figure 11. The deformed mesh without shear bands of the elastic–plastic strain-hardening plate obtained by the finite-element analysis (Hsu, *et al.*, 2021).

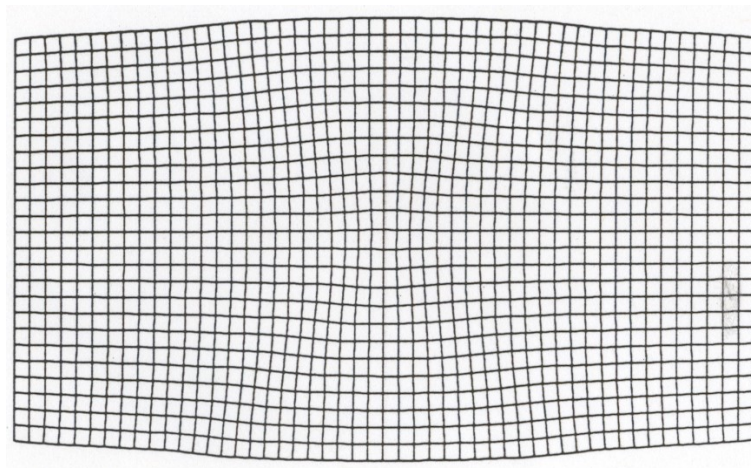


Figure 12. The deformed mesh without shear bands of the elastic–perfectly plastic plate obtained by the finite-element analysis (Hsu, *et al.*, 2021).

However, for elastic–plastic strain-softening materials, the determinant of the structural stiffness matrix $\det(\mathbf{K})$ can be equal to zero. In this analysis case, external agencies must be

applied by specified displacements instead of specified loads to obtain the analysis result for shear bands (see Figure 13).

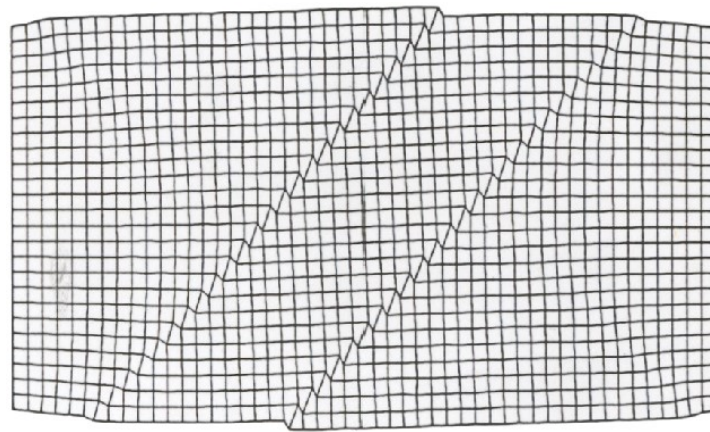


Figure 13. The deformed mesh with shear bands of the elastic–plastic strain-softening plate obtained by the finite-element analysis (Hsu, *et al.*, 2021).

Loss of symmetry

Generally, the ground surface must be leveled before foundation construction, and then the degree of soil compaction must be assessed to ensure that the foundation soil is firm or dense.

In the case of foundation soil with insufficient bearing capacity, the structure of the foundation soil will be unstable at first, and then general shear failure will occur under the loss of symmetry condition (as shown in Figures 14 and 15).



Figure 14. Tilting of a building induced by asymmetrical sliding failure of real foundation soil (Hsu and Ho, 2016).

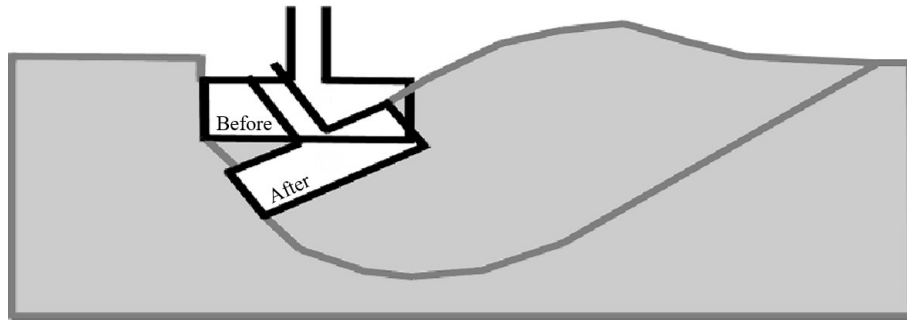


Figure 15. Schematic diagram of asymmetric sliding failure of a foundation embedded in a firm clay layer or dense sand layer.

For the triaxial compression test of a hard mudstone specimen, even if the top and bottom surfaces of the specimen are kept horizontal during the test, the prescribed vertical displacements are applied from the bottom of the specimen under the condition of axis-symmetrical conditions.

When the strain goes deep into the plastic range, localized deformations are caused by strain softening, which in turn induce shear bands. Figure 16 shows that the specimen including shear bands has obviously lost its symmetry.



Figure 16. In a triaxial compression test, the hard mudstone specimen loses symmetry as a result of plastic strain softening.

When the same triaxial compression test is performed for a soft kaolin specimen, after the strain goes deep into the plastic range, the specimen undergoes a barrel-shaped deformation

due to perfect plasticity. Figure 17 shows that the deformed specimen does not lose symmetry because it does not contain shear bands.

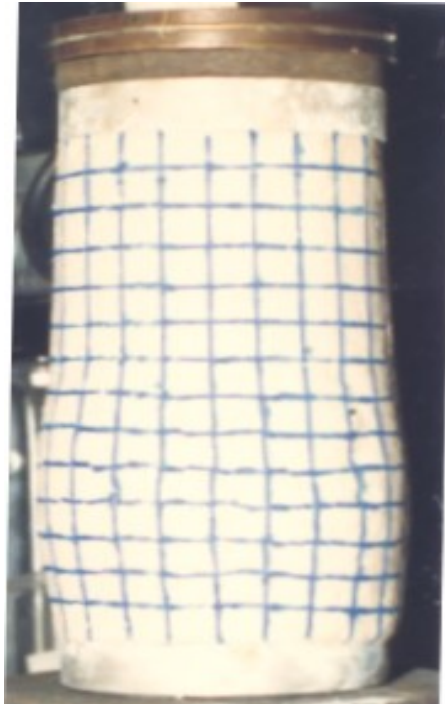


Figure 17. In a triaxial compression test, the soft kaolin specimen maintains symmetry, owing to its perfect plasticity (Hsu, 1987).

For the elastic–plastic strain-softened strip plate, under the prescribed lateral displacements at both the left and right ends, the strain energy density contours appearing in

the elastic range are symmetrical (shown in Figure 18). However, the contours of strain energy density appearing in the plastic strain-softening range are asymmetric (Figure 19).

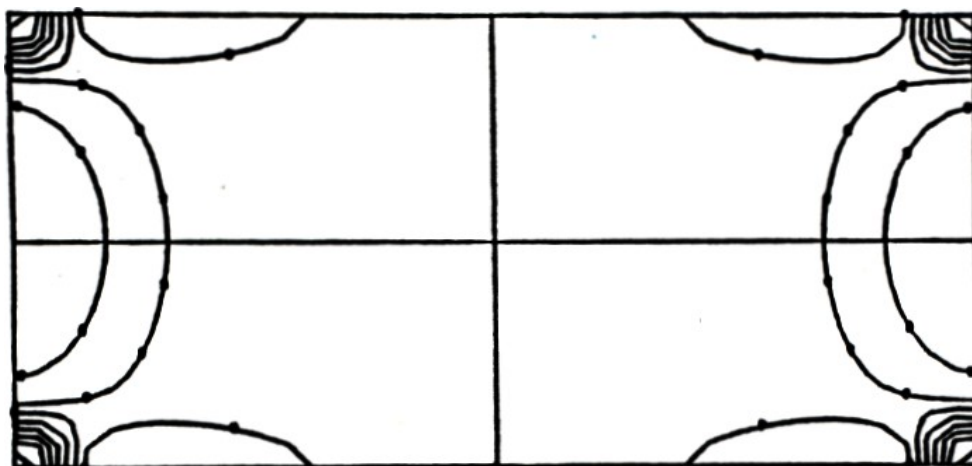


Figure 18. The symmetrical strain-energy-density contour map for the elastic range (Hsu, 1987).

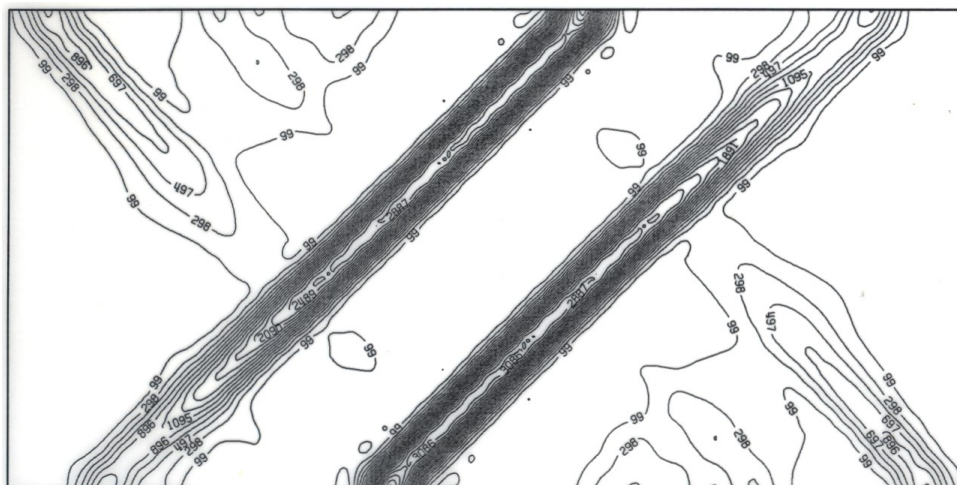


Figure 19. The asymmetrical strain-energy-density contour distribution map for the plastic strain-softening range (Hsu et al., 2017).

It can be seen that the condition for the loss of symmetry of the foundation soil or the soil specimen is the appearance of shear bands induced by plastic strain softening.

As far as the structural stiffness

matrix \underline{K} is concerned, the determinant of the structural stiffness matrix \underline{K} will be equal to zero because of the plastic strain softening, which will induce shear bands under prescribed displacements. In the elastic range, the entries of the structural stiffness matrix

\underline{K} have a symmetric condition of $k_{ij} = k_{ji}$ and in the plastic strain-softening range, the condition for the determinant of \underline{K} to be equal to zero is that the entries in the two adjacent rows of the structural stiffness matrix \underline{K} correspond, that is, $k_{mj} = k_{nj}$ for $n = m + 1$. The structure matrix is therefore asymmetric.

Comparison and Discussion of Results

- 1) In deriving the ultimate bearing capacity of the foundation, Terzaghi (1943) assumed symmetric general shear failure planes in the foundation soil under the ultimate load (see Figure 2), and the soil properties used for the foundation soil include cohesion c , angle of internal friction ϕ , and unit weight γ . The cohesion c and internal friction angle ϕ are obtained from the

perfectly plastic curves of the test results. Figure 2 shows that Terzaghi divides the whole area enclosed by the general shear failure surface into active zone I, radial shear zones II and II₁, and passive zones III and III₁. The ultimate bearing capacity Q_{ult} of the foundation is equal to twice the passive earth pressures P_p , as shown in Figure 2, that act on the \overline{ad} and \overline{bd} planes. The passive earth pressure P_p includes the passive earth pressure P_{p1} generated by the soil cohesion c , the passive earth pressure P_{p2} generated by the overburden pressure γD_f (i.e., q), and the passive earth pressure P_{p3} generated by the weight of the soil enclosed by the shear failure surface \overline{adei} . Based on the balance of the vertical components of all forces, Terzaghi obtained the ultimate bearing capacity of the foundation as:

$$\begin{aligned}
 Q_{ult} &= 2 \left(P_{p1} + P_{p2} + P_{p3} + \frac{1}{2} B c \tan \phi \right) \\
 &= B \left(c N_c + q N_q + \frac{1}{2} \gamma B N_\gamma \right), \quad \text{(Equation 13)}
 \end{aligned}$$

where N_c , N_q , and N_γ are bearing-capacity factors, where

$$\begin{aligned}
 N_q &= \frac{2P_{p2}}{\gamma D_f B} = \frac{\alpha^2}{2 \cos^2(45^\circ + \phi/2)} \quad \text{and} \\
 \alpha &= \exp(0.75\pi - \phi/2);
 \end{aligned}$$

$$N_c = \frac{2P_{ps}}{Bc} + \tan \phi = (N_q - 1) \cot \phi;$$

$$\text{and } N_y = \frac{4P_{ps}}{yB^2} = \frac{\tan \phi}{2} \left(\frac{K_{py}}{\cos^2 \phi} - 1 \right),$$

where K_{py} is equal to 10.8, 14.7, 25.0, 52.0, and 141.0, when ϕ is equal to 0° , 10° , 20° , 30° , and 40° , respectively.

2) Table 1 shows the bearing-capacity factors N_c , N_q , and N_y proposed by four scholars, Terzaghi (1943), Meyerhof (1976), Hansen (1970), and Vesic (1973), as the angle of internal friction ϕ changes. For a specific angle of internal friction angle ϕ , the N_c values proposed by Meyerhof, Hansen, and Vesic are the same, and the N_q values are

also the same. When the angle of internal friction increases from 0° to 40° , the ratios of N_c proposed by Terzaghi to those proposed by Meyerhof, Hansen, and Vesic, respectively, increased from 1.11 to 1.27. The ratios of N_q proposed by Terzaghi to those proposed by Meyerhof, Hansen, and Vesic, respectively, increased from 1.00 to 1.27. When the internal friction angle increases from 10° to 40° , the ratio of N_y proposed by Terzaghi to that proposed by Meyerhof decreases from 3.00 to 1.07, and the ratio of N_y proposed by Terzaghi to that proposed by Hansen decreases from 3.00 to 1.26, and the ratio of N_y proposed by Terzaghi to that proposed by Vesic varies between 1.00 and 0.88.

Table 1. Comparison of bearing-capacity factors provided by different studies.
 (a) N_c (Bowles, 1988)

	Angle of internal friction ϕ				
	0°	10°	20°	30°	40°
Terzaghi (1943)	5.71*	9.60	17.69	37.16	95.66
Meyerhof (1976)	5.14 (1.11)	8.34 (1.15)	14.83 (1.19)	30.13 (1.23)	75.25 (1.27)
Hansen (1970)	5.14 (1.11)	8.34 (1.15)	14.83 (1.19)	30.13 (1.23)	75.25 (1.27)
Vesic (1973)	5.14 (1.11)	8.34 (1.15)	14.83 (1.19)	30.13 (1.23)	75.25 (1.27)

Note: 1) $* = 1.5\pi + 1$;

2) The value in parentheses is the ratio of N_c proposed by Terzaghi to those proposed by Meyerhof, Hansen, and Vesic, respectively.

(b) N_q (Bowles, 1988)

	Angle of internal friction φ				
	0°	10°	20°	30°	40°
Terzaghi (1943)	1.0	2.7	7.4	22.5	81.3
Meyerhof (1976)	1.0 (1.00)	2.5 (1.08)	6.4 (1.16)	18.4 (1.22)	64.1 (1.27)
Hansen (1970)	1.0 (1.00)	2.5 (1.08)	6.4 (1.16)	18.4 (1.22)	64.1 (1.27)
Vesic (1973)	1.0 (1.00)	2.5 (1.08)	6.4 (1.16)	18.4 (1.22)	64.1 (1.27)

(c) N_γ (Bowles, 1988)

	Angle of internal friction φ				
	0°	10°	20°	30°	40°
Terzaghi (1943)	0.0	1.2	5.0	19.7	100.4
Meyerhof (1976)	0.0	0.4 (3.00)	2.9 (1.72)	15.7 (1.25)	93.6 (1.07)
Hansen (1970)	0.0	0.4 (3.00)	2.9 (1.72)	15.1 (1.30)	79.4 (1.26)
Vesic (1973)	0.0	1.2 (1.00)	5.4 (0.93)	22.4 (0.88)	109.3 (0.92)

3) When plastic strain softening induces structural instability, the asymmetric structural matrix induces general shear failure planes. Thus, the symmetric general shear failure planes set by Terzaghi before deriving the ultimate bearing capacity equation of the foundation actually do not exist. Therefore, using the Terzaghi formula to calculate the ultimate bearing capacity Q_{ult} results in overestimation of Q_{ult} by approximately two times.

4) When the rigid–perfectly plastic

model is adopted, the shear strength parameters used are all from the experimental results of the ultimate shear strength. But the general shear failure plane is induced by plastic strain softening and, therefore, the shear resistance strength will decrease from the peak value to the residual value as the strain softens. In other words, the cohesion c will be reduced from the peak value c_p to the residual value c_r , $c_r \approx 0$, and the angle of internal friction φ will also be reduced from the peak value

φ_p to the residual value φ_r . Therefore, when calculating the ultimate bearing capacity Q_{ult} using the ultimate shear resistance strength parameter, there is also an overestimation problem.

- 5) Although the safety factor used in the foundation design is as high as 2.5 to 3.0, because of the existence of the above two overestimation problems, the building is still prone to tilt or collapse after instability.
- 6) Due to the presence of highly compressible dissolved air in groundwater, Hsu *et al.* (2022) found that saturated clay as defined by traditional scholars is actually only

seemingly saturated clay. When the foundation is embedded in a seemingly saturated clay layer, at the moment when the vertical pressure increment is applied, the dissolved air in the pore water of the clay layer will be instantly compressed, resulting in an immediate settlement (Hsu *et al.*, 2021). Therefore, the triaxial compression tests for saturated clay specimens performed under unconsolidated and undrained conditions with no volume change do not actually exist. Since such test conditions do not exist, therefore, the test results of $S_w = c$ and $\varphi = 0$ shown in Figure 20 adopted by Chi and Lin (2020) have no substantial meaning.

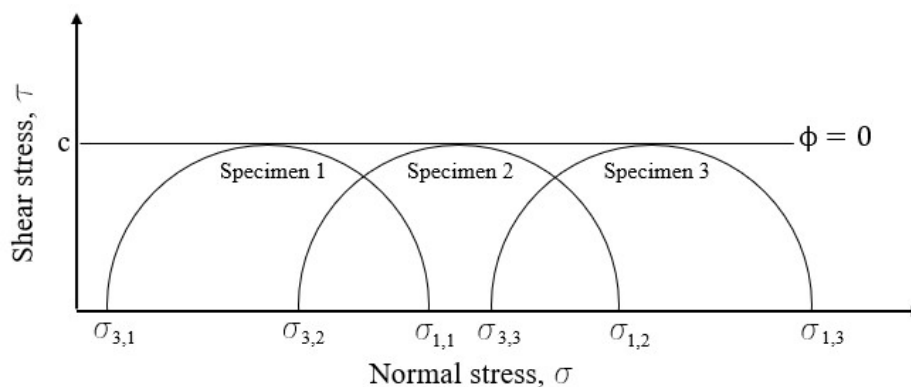


Figure 20. Typical triaxial compression test results under unconsolidated and undrained test conditions for traditional saturated clay specimens.

- 7) When shear bands are induced after the localized deformations occur, the plastic zones only exist inside the shear bands, while the elastic

zones exist outside the shear bands, as shown in Figure 19.

- 8) When the elastic–perfectly plastic model is adopted, plastic zones spread to both sides of the foundation soil, as shown in Figure 21. Figure 22 shows the distribution of the elastic zones and the plastic zones obtained from finite-element analysis. It can be seen from Figure 22 that the elastic zones and plastic zones are also symmetrically dis-

tributed. Since the simplified perfectly plastic model is used to replace the plastic strain-softening model in the analysis, when asymmetric shear bands cannot be obtained, the elastic zones that should originally exist outside the shear bands are largely turned into plastic zones. Therefore, the results of this analysis obviously do not meet the actual needs of general shear failure of foundations.

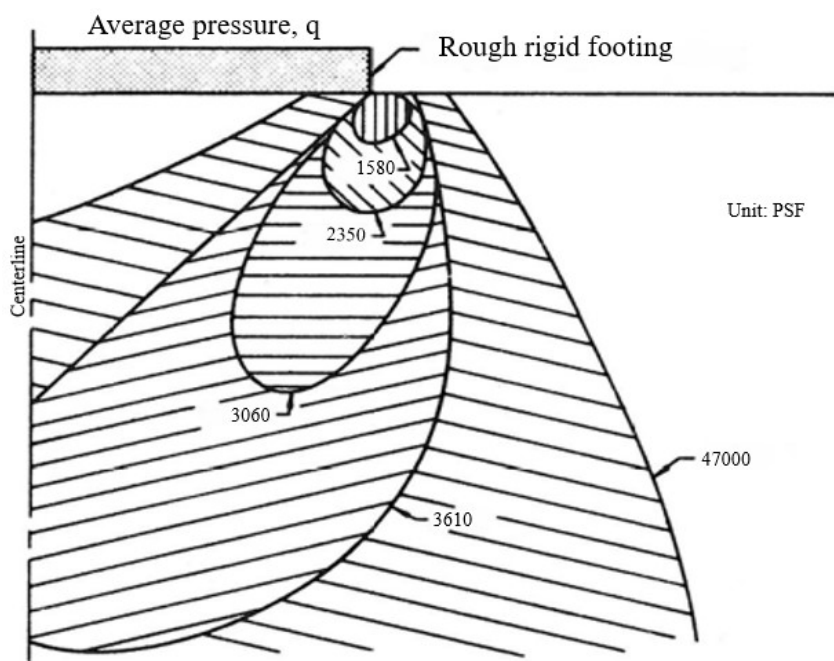


Figure 21. Spread of plastic zones obtained by finite-element analysis using elastic–perfectly plastic model (Chen, 1975).

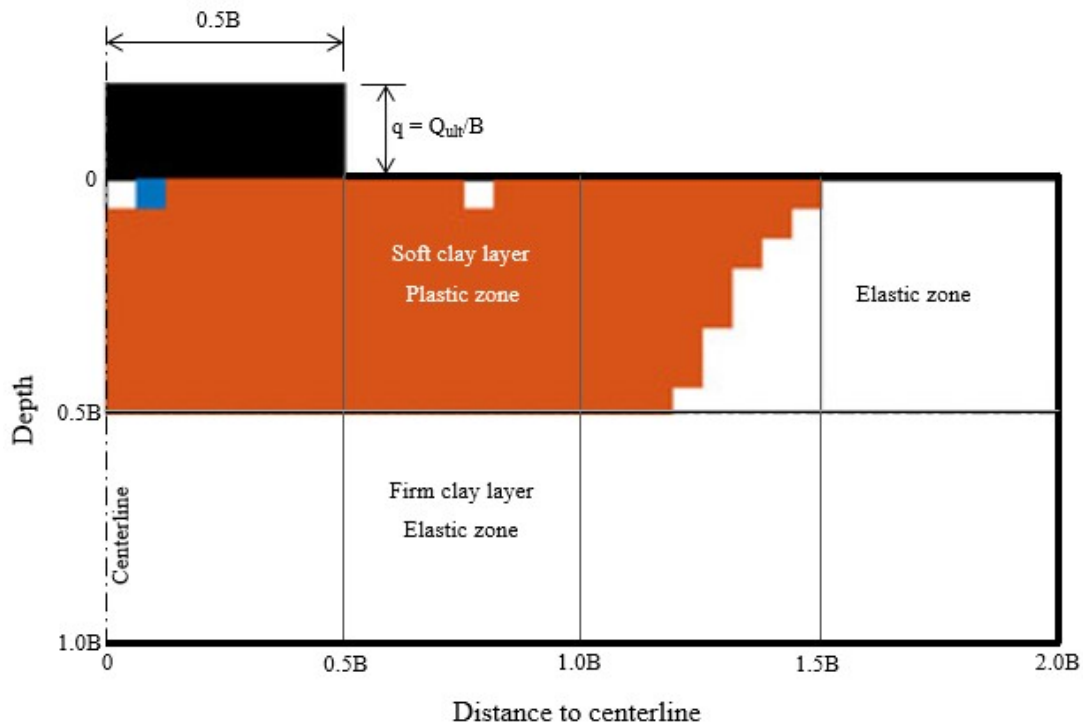


Figure 22. Elastic zones and plastic zones obtained by finite-element analysis using elastic–perfectly plastic model (reproduced from Chi and Lin, 2020).

Conclusions and Suggestions

Current literature reveals that shear bands only appear under plastic strain softening, and shear-band solutions under structural instability conditions have also been demonstrated to be obtained by prescribed displacements. Therefore, based on the research results of this paper, the following four conclusions are obtained:

1) Based on the elastic–plastic strain-softening constitutive equation, shear-band solutions come from the determinant of the struc-

tural matrix \underline{D}^{ep} being equal to zero. Therefore, shear-band solutions can be obtained by the finite-element method under prescribed displacements.

2) In the case that the initial structure matrix is symmetric, when the strain goes deep into the plastic range, the structure matrix \underline{D}^{ep} will lose its symmetry when its determinant is equal to zero. Therefore, the general shear failure plane must not be set to be symmetrical under the ultimate load for a foundation embedded in a firm clay layer or dense sand layer.

- 3) When the general shear failure plane is set, once the strain-softening model is replaced by the perfectly plastic model, the foundation soil will remain perfectly plastic when it should be strain-softened, and then it will still maintain symmetry when it should be lost. Finally, the problem of overestimating the ultimate bearing capacity of foundations also arises.
 - 4) When the shear band appears, the plastic zones will only exist locally inside the shear bands, and all the outside of the shear bands are elastic zones. If the perfectly plastic model is adopted to replace the strain-softening model in the analysis, then, in the case that the shear band cannot be induced, most of the elastic zones that should have existed outside the shear bands will be incorrectly turned into plastic zones.
- 2) The design code should completely exclude the ultimate bearing capacity equation for a foundation derived based on the perfectly plastic model, so as to avoid the collapse of the building due to misuse by the technician, and to ensure the safety of all foundations within the service life.

References

- Bolton, M. D., Lau, C. K., "Vertical bearing capacity factors for circular and strip footings on Mohr-Coulomb soil," *Canadian Geotechnical Journal*, Vol. 30, No. 6, pp. 1024–1033, 1993.
- Bowles, Joseph E., *Foundation Analysis and Design*, 4th Edition, McGraw-Hill International Editions, Civil Engineering Series, pp. 187-190, 1988.
- Chen, W. F., *Limit Analysis and Soil Plasticity*, Elsevier Scientific Pub. Co.: Amsterdam, The Netherlands; New York, NY, USA, 1975.
- Chi, Chao-Ming and Zheng-Shan Lin, "The Bearing Capacity Evaluations of a Spread Footing on Single Thick Stratum or Two-Layered Cohesive Soils," *Journal of Marine Science and*

In view of the above four conclusions, the authors suggest:

- 1) In future, analysis of the ultimate bearing capacity of foundations must be more rigorous, especially when it is clear that general shear failure will not occur in the perfectly plastic model, and such a model should no longer be used to analyze the ultimate bearing capacity of the foundation.

- Engineering*, Vol. 8, No.11, pp. 853, 2020.
- Das, Braja M., *Principles of Foundation Engineering*, 7th Edition, 1983.
- Davis, E. H., Booker, J. R., "The bearing capacity of strip footings from the standpoint of plasticity theory," *1st Australia-New Zealand Conference on Geomechanics*, Melbourne, 1971.
- Griffiths, D. V., "Computation of bearing capacity factors using finite elements," *Geotechnique*, Vol. 32, No. 3, pp. 195–202, 1982.
- Hansen, J. B., "A Revised and Extended Formula for Bearing Capacity," *Danish Geotechnical Institute Bulletin*, No. 28, Copenhagen pp. 5-11, 1970.
- Hsu, Tse-Shan, *Capturing Localizations in Geotechnical Failures*, Ph.D. Dissertation, Civil Engineering in the school of Advanced Studies of Illinois Institute of Technology, 1987.
- Hsu, Tse-Shan, Chang-Chi Tsao, and Chihsen T. Lin, "Localizations of Soil Liquefactions Induced by Tectonic Earthquakes," *The International Journal of Organizational Innovation*, Vol.9, No. 3, Section C, pp. 110-131, 2017.
- Hsu, Tse-Shan, Cheng-Chieh Ho, "Shear Banding Induced Seismic Building Tilting Failure and Its Control," *International Journal of Organizational Innovation*, Vol. 9, No. 1, pp. 264-281, 2016.
- Hsu, Tse-Shan, Lin-Yao Wang, Da-Jie Lin, and Tsai-Fu Chuang, "Effect of Dissolved Air in Water on Consolidation Test Results," *The International Journal of Organizational Innovation*, Volume 14 Number 3, January, 2022.
- Tse-Shan Hsu, Yi-Ju Chen, Zong-Lin Wu, Yi-Lang Hsieh, Ji-ann-Cherng Yang, Yi-Min Huang, "Influence of Strain Softening and Shear-band Tilting Effect on the Maximum Earth Pressure of Retaining Walls," *International Journal of Organizational Innovation*, Vol. 14, No. 1, pp. 45-86, 2021.
- McCarthy, David F., *Essential of Soil Mechanics and Foundations: Basic Geotechnics*, 7th Edition, Pearson Prentice Hall, pp. 346-349, 2007.
- Meyerhof, G. G., "Ultimate bearing

- capacity of footings on sand layer overlying clay,” *Canadian Geotechnical Journal*, Vol. 11, pp. 223-229, 1974.
- Peng, Ming-Xiang and Hong-Xi Peng, “The ultimate bearing capacity of shallow strip footings using slip-line method,” *Soils and Foundations*, Website: <https://www.researchgate.net/journal/Soils-and-Foundations-Tokyo-1881-1418>, 2019.
- Prandtl, L. “Über die Härte, plastischer Körper, (On the Hardness of Plastic Bodies),” *Nachr. Kgl. Ges Wiss Göttingen, Math-Phys. Kl.*, pp. 74, 1920.
- Prevost, J. H., *Soil Stress-Strain-Strength Models Based on Plasticity Theory*, Ph.D. Dissertation, Department of Civil Engineering of Stanford University, 1974.
- Reissner, H., On the determination of earth pressures during earthquakes.” *Proceeding of World Engineering, Congress*, Okabe, S., Vol. 9, pp. 177-185, 1924.
- Rice, James R., “The Localization of Plastic Deformation,” in *Theoretical and Applied Mechanics, Proceedings, 14th International Congress of Theoretical Applied Mechanics*, ed. Koiter, W. T. , North-Holland, Inc., Amsterdam, pp. 207-220, 1977.
- Rudnicki, J. W., and Rice, J. R., “Conditions for the Localization of Deformation in Pressure-Sensitive Dilatant Materials,” *Journal of the Mechanics and Physics of Solids*, Vol. 23. pp. 371-394. 1975.
- Sokolovskii, V. V., *Statics of Granular Media*, Pergamon Press, Oxford, UK, 1965.
- Vesic, A. S., Analysis of Ultimate Loads of Shallow Foundation,” *Journal of Soil Mechanics and Foundation Engineering, ASCE*, Vol. 99, SM1, pp. 45-73, 1973.
- You, Qi-Heng, *Essentials of Soil Mechanics*, Dashing Publishing Company, p. 340, 1974.